

Tu\_P02\_11

## Speeding up a Mass-Lumped Tetrahedral Finite-Element Method for Wave Propagation

W. Mulder<sup>1,2\*</sup>, S. Geevers<sup>3</sup>, J. Van der Vegt<sup>4</sup>

<sup>1</sup> Shell Global Solutions International BV; <sup>2</sup> Delft University of Technology; <sup>3</sup> Universität Wien;

<sup>4</sup> University of Twente

### Summary

---

Mass-lumped finite elements on tetrahedra offer more flexibility than their counterpart on hexahedra for the simulation of seismic wave propagation, but there is no general recipe for their construction, unlike as with hexahedra. Earlier, we found new elements up to degree 4 that have significantly less nodes than previously known elements by sharpening the accuracy criterion. A similar approach applied to numerical quadrature of the stiffness matrix provides a speed improvement in the acoustic case and an additional factor 1.5 in the isotropic elastic case. We present numerical results for a homogeneous and heterogeneous isotropic elastic test problem on a sequence of successively finer meshes and for elements of degrees 1 to 4. A comparison of their accuracy and computational efficiency shows that a scheme of degree 4 has the best performance when high accuracy is desired, but the one of degree 3 is more efficient at intermediate accuracy.

## Introduction

Seismic wavefield modelling with the finite-element method can be a better alternative for the finite-difference method in the presence of rough topography or large geological contrasts. The spectral element method (SEM) on hexahedra (Komatitsch and Tromp, 1999) is popular among seismologists. Tetrahedra offer more flexibility in meshing complex geological models. Unlike as for the SEM, there is no closed-form expression for the construction of higher-degree elements, which are usually more efficient than the lower-order ones. Elements of degree 2 (Mulder, 1996) and 3 (Chin-Joe-Kong et al., 1999) have been known for some time, but are quite expensive because they have about 2.5 times as many nodes as the standard elements for those degrees. The discontinuous Galerkin method, incidentally, leads to a similar cost increase over the standard element because of the additional fluxes that handle continuity across elements and the block-diagonal mass matrix. More recently, Geevers et al. (2018a,b) found new mass-lumped elements of degree 2, 3 and 4 by refining the accuracy conditions. The new elements are more efficient than the older ones because they have less nodes and allow for larger time steps.

Here, we present a further acceleration of the method by applying tailor-made numerical quadrature instead of exact evaluation to the computation of the stiffness matrix times the solution vector. After a brief review of the method, we compare exact and approximate evaluation of the stiffness matrix for a homogeneous elastic problem and observe the expected convergence rates when refining the mesh. We then repeat the exercise for an inhomogeneous example.

## Method

In the Galerkin finite-element approximation of the wave equation in second-order form, the spatial derivatives lead to a product of a stiffness matrix and a vector containing the coefficients of the solution expansion, whereas the temporal derivatives involve a mass matrix. Inversion of the sparse mass matrix slows down the time stepping, but can be avoided by replacing the matrix by a diagonal one that is easily inverted. Mass lumping diagonalizes the mass matrix by taking row sums and placing them on the diagonal. Stability for explicit time stepping requires that the diagonal elements are strictly positive. Accuracy requires that the lumped values, apart from a volume factor, corresponds to quadrature weights that are exact for polynomials of sufficiently high degree. In the SEM with Legendre-Gauss-Lobatto nodes for polynomials of degree  $p$ , mass lumping in 1D is equivalent to exact quadrature with positive integration weights up to degree  $2p - 1$ . In 2D on triangles, mass lumping does not have this property, except for the simplest linear element of degree 1. For degree 2, some of the nodes have zero weights. Positivity can be restored by an adding a bubble function that is zero on the triangle's edges and one at the centroid. Since the bubble function is of degree 3, this means that the set of polynomial basis functions of degree  $p = 2$  is augmented by a polynomial of degree  $p' = 3$  in the interior. With this choice and the accuracy requirement that quadrature be exact for polynomials of degree  $p + p' - 2$  (Ciarlet, 1978), positive weights are obtained—also known as Simpson's rule on the triangle. For degree 3, the product of the bubble function and degree-1 polynomials should be added to the set of basis functions (Cohen et al., 1995). The generalization to tetrahedra requires bubble functions on the faces, similar to those on triangles, as well as a bubble function in the interior, which is zero on the faces and edges and one at the centroid (Mulder, 1996; Chin-Joe-Kong et al., 1999).

The accuracy requirement of exactness for degree  $p + p' - 2$  has a self-defeating character: positivity requires an increased  $p' > p$  but a higher  $p'$  makes it more difficult to find node positions and quadrature weights with the desired properties. On tetrahedra, only elements up to degree 3 were found, with about 2.5 times more nodes than the standard elements. Geevers et al. (2018a,b) could reduce the number of extra nodes by a sharper accuracy condition: quadrature should be exact for  $P_{p-2} \otimes \tilde{U}$  with  $P_{p-2}$  the space spanned by polynomials up to degree  $p - 2$  and, for degrees  $p = 2$  and 3,  $\tilde{U} = P_p \oplus (b_f P_{p_f-3}) \oplus (b_i P_{p_i-4}) \subset P_{p'}$ , involving polynomials up to degree  $p$  in the edges, the product of the cubic face bubble functions  $b_f$  with polynomials up to degree  $p_f - 3$  and the product of the degree-4 interior bubble function  $b_i$  with polynomials up to degree  $p_i - 4$ . As  $\tilde{U}$  is a smaller subset of  $P_{\max(p, p_f, p_i)}$ , the resulting new elements have less nodes, allow for larger time steps, and are therefore more efficient than the ones previously know. Also, three new elements of degree 4 were found where instead of just  $P_{p_f-3}$  and

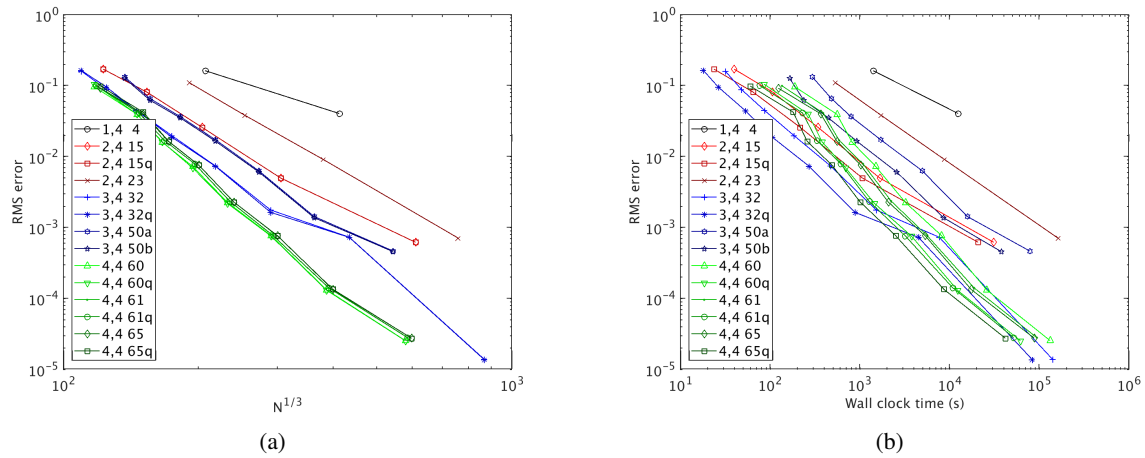


**Figure 1** RMS errors for a homogeneous elastic problem as a function of (a) the cube root of the number of scalar degrees of freedom  $N$  and (b) the elapsed wall clock time.

$P_{p_i-4}$ , we have combinations of lower-degree polynomials and bubble functions. We can extend this idea to numerical quadrature of the stiffness matrix: quadrature should then be exact for  $P_{p-1} \otimes D\tilde{U}$ , with  $D\tilde{U}$  the space containing the spatial derivatives of elements in the earlier  $\tilde{U}$ . For the acoustic wave equation, exact on-the-fly evaluation for models that are piecewise constant per element required six matrix-vector multiplication with square matrices of the size of the number of nodes in each dimension (Mulder and Shamasundar, 2016). The 6 matrices can be pre-computing on the reference element with exact quadrature. Numerical quadrature involves 6 non-square matrices, with one dimension equal the number of nodes per element and the other equal to the smaller number of quadrature nodes. This speeds up the method. For the isotropic elastic wave equation, another factor 1.5 is gained, while accuracy is preserved (Geevers et al., 2019). Also, the model does not have to be piecewise constant per element. In the next section, we examine the performance of this method in terms of formal accuracy and actual run times.

## Results

### Homogeneous isotropic elastic problem

As a first test, we consider the isotropic elastic wave equation for a model with a constant density of  $2\text{g/cm}^3$ , P-velocity of  $2\text{km/s}$  and S-velocity of  $1.2\text{km/s}$ . A vertical force source at the centre of the domain of size  $[-2, 2] \times [-1, 1] \times [0, 2]\text{km}^3$  has a 7-Hz zero-phase Ricker wavelet. 56 receivers are placed between  $(-1375, 200, 800)\text{m}$  and  $(+1375, 200, 800)\text{m}$  at a 50-m spacing. Free-surface boundary conditions are imposed all around. The computations starts at about  $-0.29\text{s}$ , when the wavelet has an amplitude around machine precision, and ends at  $0.6\text{s}$ , before reflections from the boundaries reach the receivers. Figure 1a shows the root-mean-square errors in the recorded displacement data, measured per trace, scaled by the square root of the energy per trace, and averaged over the 3 components and all traces. We considered a sequence of unstructured meshes. The number of nodes involved in the finite-element discretization is denoted by  $N$ . The total number of degrees of freedom for the 3 displacement components is  $3N$ . The average element size scales with  $N^{-1/3}$ . The set of numbers in the legend are: the degree  $p$  of the element, the order of the time stepping scheme, which is 4 in all cases, and the number of nodes per element. The extra symbol q denotes numerical quadrature of the stiffness matrix. The expected convergence rate is proportional to  $(N^{-1/3})^{p+1}$  for degree  $p$  and is met on average. We observe that the formal convergence rates, one higher than the degree, are met and that numerical quadrature for the spatial operators does not make much difference in the resulting accuracy.

Figure 1b plots the errors as a function of the observed run time with an openMP implementation on 24 cores of two Intel<sup>®</sup> 2.50-GHz Xeon<sup>®</sup> E5-2680 v3 cpus (Haswell). Clearly, the newer schemes with less nodes as well as numerical quadrature for the spatial operators are more efficient. The degree-4 element

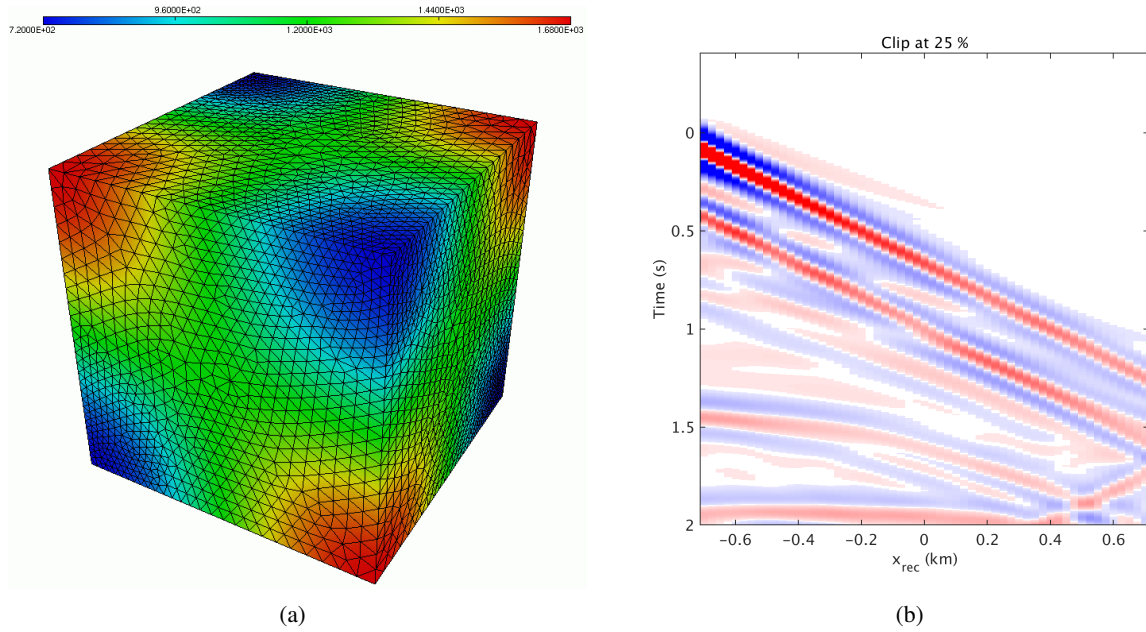


**Figure 2** (a) S-velocity model displayed on the surface of the unstructured mesh. (b) Seismic data, clipped at 25% of the maximum amplitude.

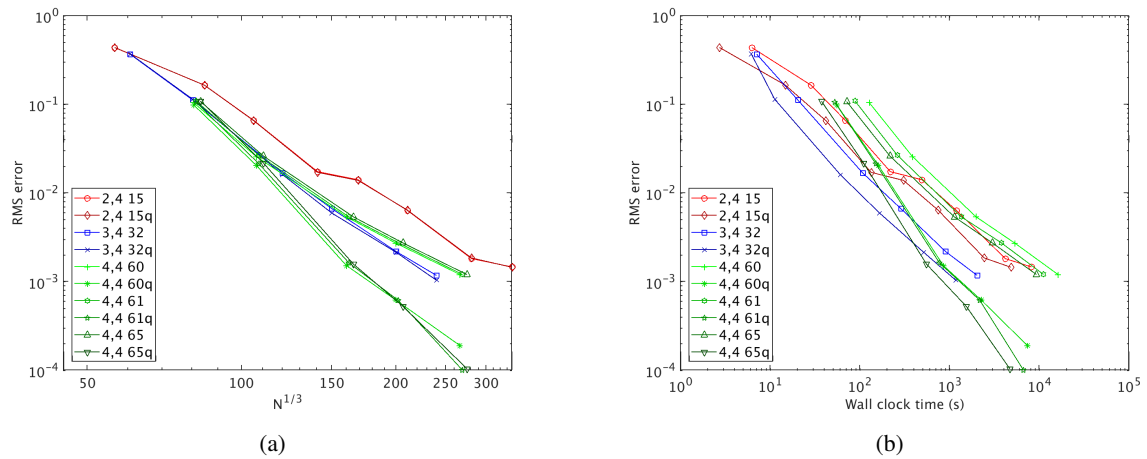


**Figure 3** RMS errors for an inhomogeneous elastic problem as a function of (a) the cube root of the number of scalar degrees of freedom  $N$  and (b) the elapsed wall clock time.

with 65 nodes is more efficient than the ones with 60 or 61 nodes, even though it employs more nodes per element, because it allows for a larger time step. Overall, the element of degree 3 with 32 nodes appears to be an attractive choice.

### Inhomogeneous elastic problem

The computational domain has a size  $[-1, 1] \times [-1, 1] \times [-1, 1] \text{ km}^3$  with free-surface boundary conditions imposed all around. The P-velocity is  $v_p = 2 + 0.8 \cos(\pi X) \cos(\pi Y) \cos(\pi Z) \text{ km/s}$  with  $X = (x - x_{\min}) / (x_{\max} - x_{\min})$  and similarly for  $Y$  and  $Z$ . The S-velocity is given by  $v_s = 0.6 v_p$  and the density follows from Gardner's rule (Gardner et al., 1974). A unit vertical force source located at  $x_s = -800 \text{ m}$ ,  $y_s = 0 \text{ m}$  and  $z_s = -500 \text{ m}$  has a Ricker wavelet with a 5-Hz peak frequency. Receivers are placed at  $x_r$  between  $-700$  and  $+700 \text{ m}$  at a 25-m spacing, whereas  $y_r = 0$  and  $z_r = -500 \text{ m}$ . The computations start at about  $-0.41 \text{ s}$  to have the wavelet peak at zero time and end at  $2 \text{ s}$ . Figure 2a shows one of the coarser meshes with the S-velocity, defining the scaling field, superimposed. Figure 2b displays the recorded data. We chose such a simple problem to avoid potential errors caused by imperfect absorbing boundary

condition or by corner singularities in non-trivial topography or hard subsurface contrasts.

Figure 3a shows the estimated root-mean-square errors as a function of the number of scalar degrees of freedom, one-third of the total unknowns. Since we do not have the exact solution, we have used the results for a still finer mesh as reference. The legend is similar to the one in Figure 1. Power-law fits show that the orders agree with the expected rates of  $p + 1$ , where  $p$  is the degree of the scheme, if numerical quadrature of the stiffness matrix is applied, indicated by the  $q$  in the legend. If not, the model parameters are set to be piecewise constant per element and we adopt the values at the centroids of the tetrahedra. The graph shows that the schemes of degree 2 and 3 still can keep up, but convergence for the three schemes of degree 4 stagnates with a power of about 3.5 instead of the expected 5, becoming worse than the scheme of degree 3. Figure 3b shows the errors as function of the elapsed time on 24 cores. The schemes of degree 4 without numerical quadrature of the stiffness matrix clearly lose out. With that quadrature, the scheme of degree 3 (3,4 32q) appears to be the most attractive. Only at high accuracy, degree 4 (4,4 65q) starts to win.

## Conclusions

A sharper accuracy criterion enabled the construction of set of new tailor-made quadrature rules for evaluating the stiffness matrices in mass-lumped tetrahedral finite elements. This accelerates the simulation of elastic wave propagation by at least a factor 1.5. If model parameters vary smoothly per element, the formal accuracy is preserved, which is not true if an effective value at the centroid in combination with exact evaluation is chosen. In practical computations at intermediate accuracy, the scheme of degree 3 can be the best choice. Only at high accuracy, the scheme of degree 4 with 65 nodes may perform better.

## References

- Chin-Joe-Kong, M.J.S., Mulder, W.A. and van Veldhuizen, M. [1999] Higher-order triangular and tetrahedral finite elements with mass lumping for solving the wave equation. *Journal of Engineering Mathematics*, **35**, 405–426.
- Ciarlet, P.G. [1978] *The finite element method for elliptic problems*. North-Holland.
- Cohen, G., Joly, P. and Tordjman, N. [1995] Higher order triangular finite elements with mass lumping for the wave equation. In: Cohen, G., Bécache, E., Joly, P. and Roberts, J.E. (Eds.) *Proceedings of the Third International Conference on Mathematical and Numerical Aspects of Wave Propagation*. SIAM, Philadelphia, 270–279.
- Gardner, G.H.F., Gardner, L.W. and Gregory, A.R. [1974] Formation velocity and density—The diagnostic basics for stratigraphic traps. *Geophysics*, **39**(6), 770–780.
- Geevers, S., Mulder, W.A. and van der Vegt, J.J.W. [2018a] New continuous mass-lumped finite elements for 3D wave propagation. In: *80th EAGE Conference and Exhibition 2018, Extended Abstracts*.
- Geevers, S., Mulder, W.A. and van der Vegt, J.J.W. [2018b] New higher-order mass-lumped tetrahedral elements for wave propagation modelling. *SIAM Journal on Scientific Computing*, **40**(5), A2830–A2857.
- Geevers, S., Mulder, W.A. and van der Vegt, J.J.W. [2019] Efficient quadrature rules for computing the stiffness matrices of mass-lumped tetrahedral elements for linear wave problems. *SIAM Journal on Scientific Computing*. Revision submitted.
- Komatitsch, D. and Tromp, J. [1999] Introduction to the spectral-element method for 3-D seismic wave propagation. *Geophysical Journal International*, **139**(3), 806–822.
- Mulder, W.A. [1996] A comparison between higher-order finite elements and finite differences for solving the wave equation. In: Désidéri, J.A., LeTallec, P., Oñate, E., Périaux, J. and Stein, E. (Eds.) *Proceedings of the Second ECCOMAS Conference on Numerical Methods in Engineering*. John Wiley & Sons, Chichester, 344–350.
- Mulder, W.A. and Shamasundar, R. [2016] Performance of continuous mass-lumped tetrahedral elements for elastic wave propagation with and without global assembly. *Geophysical Journal International*, **207**(1), 414–421.